Indian J. Phys. **76B** (6), 731–736 (2002)

I J P B
— an international journal

Theoretical studies of radiations from equilateral triangular microstrip antenna on ferrite substrate

Vishwas Bhardwaj†, Vijay Kr Tiwari, J S Saini, K B Sharma† and D Bhatnagar*

Microwave Laboratory, Department of Physics, University of Rajasthan, Jaipur-302 004, India

†Department of Physics, S S Jain Subodh P G College, Jaipur-302 004, India

E-mail dbhatnagar_2000@rediffmail com

Received 12 August 2002, accepted 7 October 2002

Abstract Cavity model in conjunction with model expansion technique is applied to determine the radiation behavior of an Equilateral Triangular Microstrip Antenna (ETMA) printed on ferrite substrate. This theoretical study is carried out in TM_{11} mode of excitation, which predicts a larger bandwidth of an Equilateral Triangular Microstrip Antenna in comparison to a similar antenna built on pure dielectric substrate *i.e.* substrate having no magnetic properties Quality factor, directivity and bandwidth of this antenna are computed as a function of bias magnetic field strength. Impedance characteristics and far field radiation patterns of this antenna are also computed theoretically as a function of bias field strength For better understanding, the radiation characteristics of this structure are compared with that of similar structure designed on low permittivity pure dielectric substrate

Keywords : Microstrip antenna, ferrites, circular polarization and radiation properties.

PACS Nos. : 84.40.Ba, 75.50.Gg, 85 70 Gc

1. Introduction

Ferrites and other magnetic materials have been extensively applied in several microwave devices such as phase shifters, isolators, circulators, tunable filters, delay lines *etc.* Ferrite materials have a significant amount of anisotropy at microwave frequencies [1]. This anisotropy gets induced by applying external d.c. magnetic field in ferrites or gyrotropic materials and brings about non-reciprocal behavior in them. For many years, these properties of ferrite materials have found application in non-reciprocal and controllable microwave components. More recently, with the availability of low loss commercial microwave ferrite substrates and advances in thin film technology, unbiased ferrite materials have been used in printed antenna applications to provide loading for antenna size reduction [2].

Microstrip antennas on pure dielectric substrate have been extensively analysed in these years due to their advantages over bulky antennas [3]. The bandwidth of such antennas in GHz frequency range is typically of the order of 1 percent and they have not been tried at lower range of ultra high frequency (UHF) due to their large size considerations. Owing to the high value of effective permeability of ferrite substrates, microstrip antennas designed on a ferrite substrate can operate as low as 0.5 GHz without any large constraint [4]. Patch antennas on ferrite substrate offer greater agility in controlling the radiation characteristics of the antenna. Their inherent anisotropy and nonreciprocal properties permit variable frequency tuning [5] and antenna polarisation diversity [6]. External biasing of ferrite substrate allows beam stearing [7], pattern shape control and radar cross section (RCS) control [8] by forcing the ferrite material in to the cut-off state [9]. The material properties of ferrites are mainly controlled by direction and strength of external applied magnetic field thus enabling control of various antenna radiation and scattering characteristics.

*Corresponding Author

This paper describes theoretically the radiation characteristics of an equilateral triangular microstrip antenna (ETMA) printed upon a typical ferrite substrate $Ni_{1.062}Co_{0.02}Fe_{1.948}O_4$. Design requirements and substrate characteristics considered for theoretical analysis are listed in Table 1.

Table 1. Design requirements and substrate characteristics of ferrite substrate $Ni_{1.062}Co_{0.02}Fe_{1.948}O_4$

1	Design frequency (fr)	1.75 GHz
2	Relative permittivity (ε_r)	14.78
3	Relative permeability (μ_r)	14.74
4	Dielectric loss tangent (tan δe)	0.0476
5	Magnetic loss tangent (tan δm)	0.0062
6	Saturation magnetization ($\mu_0 M_s$)	0.3 Tesla
7	Patch dimension (a)	0.03 meter
8	Substrate thickness (h)	0.002 meter

2. Theoretical considerations

Geometry and coordinate system of an equilateral triangular microstrip antenna on ferrite substrate are shown in Figures 1(a) and 1(b). The triangular patch with side lengths $a = \frac{2\lambda_d}{\sqrt{\varepsilon_r}}$ where λ_d is lying in X-Y plane

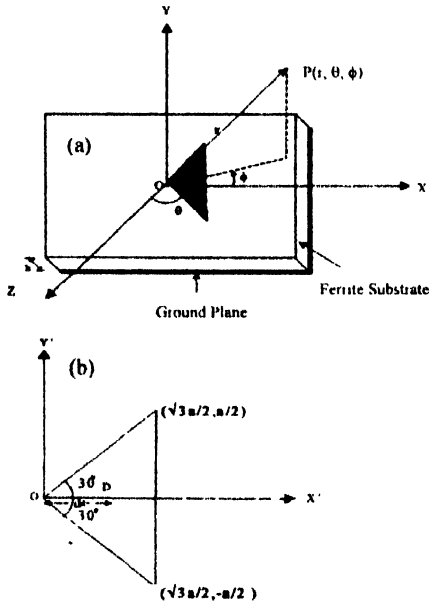

Figure 1. (a) Geometry of ETMA structure on ferrite substrate and (b) ETMA structure with coordinate system.

as shown in Figure 1(b). The electric field within the substrate has only a z-component while magnetic field have both x- and y-components. Since the substrate thickness $h \ll \lambda_0$, the field within the substrate do not vary along the z-direction and component of current; normal to the edge of antenna approaches to zero at the edges. This implies that the present structure supports TM_{mn} modes. With these assumptions, antenna is considered as a triangular resonator with magnetic sidewalls bounded at its top and bottom by electric walls.

The electric field inside the cavity is considered as same as [10] *i.e.*

$$E_z = j\omega\mu \sum_{n=0}^{\infty}\sum_{m=n}^{\infty} A_{mn}\left[\left\{\cos\left(\frac{2\pi x}{\sqrt{3}a}+\frac{2\pi}{3}\right)l\right\}\right.$$
$$\times\left\{\cos\left(\frac{2\pi(m-n)y}{3a}\right)\right\}+\left\{\cos\left(\frac{2\pi x}{\sqrt{3}a}+\frac{2\pi}{3}\right)m\right\}$$
$$\times\left\{\cos\left(\frac{2\pi(n-l)y}{3a}\right)\right\}+\left\{\cos\left(\frac{2\pi x}{\sqrt{3}a}+\frac{2\pi}{3}\right)n\right\}$$
$$\left.\times\left\{\cos\left(\frac{2\pi(l-m)y}{3a}\right)\right\}\right]. \quad (1)$$

Here, m, n and l are integers which are never zero simultaneously and satisfy the condition $m + n + l = 0$. By using standard method [10], the expression of mode amplitude coefficient A_{mn} is derived. The magnetic field components inside the cavity can be determined by simplifying Maxwell's equations in the presence of suitable boundary conditions.

The grounded ferrite can support various guided modes. These propagating modes get affected in the presence of applied magnetic bias field [11]. When the propagation of electromagnetic waves takes place along the direction of applied magnetic bias field, two plane wave modes namely left hand circularly polarised (LHCP) mode and right hand circularly polarised (RHCP) mode may exist. The magnetic properties of ferrite substrate affect both these modes. The effect on LHCP mode is weaker while on RHCP mode, the effect is stronger. In the present communication, the propagation is considered parallel to applied bias field therefore effective permeability of substrate (μ_{eff}) will be given by [1] :

$$\mu_{eff} = \mu \pm k \quad (2)$$

with $$\mu = \mu_0\left(\frac{1+\omega_0\omega_m}{\omega_0^2-\omega^2}\right) \quad (3)$$

and $$k = \mu_0\left(\frac{\omega\omega_m}{\omega_0^2-\omega^2}\right), \quad (4)$$

ω_0 and ω_m are the precession and forced precession frequencies respectively and may be defined as

$$\omega_0 = \mu_0\gamma H_0,\ \omega_m = \mu_0\gamma M_s \text{ and } \omega = 2\pi fr.$$

Here, μ_0 is the free space permeability. Applied DC magnetic bias field (H_0) and saturation magnetization ($\mu_0 M_s$) are

considered in Amp/m and Tesla respectively. Gyromagnetic ratio γ is considered equal to 1.75×10^{11} rad/sec Tesla.

The effective permeability for right hand circular polarisation (RHCP) and left hand circular polarisation (LHCP) modes are calculated using following relations.

$$\mu_{effL} = \mu_0\left[1+\frac{\omega_m}{\omega_0+\omega}\right] \quad \text{for LHCP wave,} \tag{5}$$

$$\mu_{effR} = \mu_0\left[1+\frac{\omega_m}{\omega_0-\omega}\right] \quad \text{for RHCP wave.} \tag{6}$$

In Figure 2, the variation of effective permeability (μ_{eff}) with applied magnetic bias field (H_0) is shown for both RHCP and LHCP modes. As shown in this figure, effective permeability of substrate decreases with increase in applied

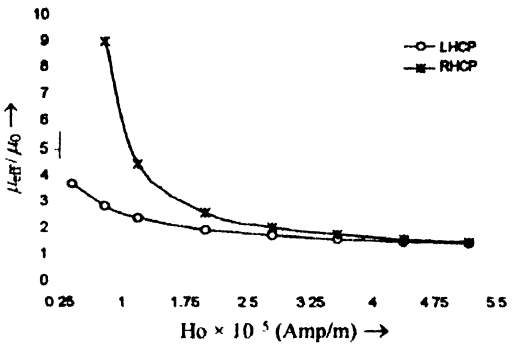

Figure 2. Variation of effective permeability of substrate with applied bias field

bias magnetic field. For RHCP mode, as soon as applied bias approaches below 4.98×10^4 Amp/meter, μ_{eff} becomes negative. This is the 'off switch' condition. For LHCP mode, μ_{eff} remain positive for all values of applied bias field. On reversing the direction of bias field, the value of effective permeability (μ_{eff}) of RHCP and LHCP modes interchanges among themselves. This indicates that in these operation modes, values of different radiation parameters of antenna will also interchange among themselves for a given range of bias field.

The resonance frequency (f_r) and input impedance (Z_{in}) of considered equilateral triangular microstrip antenna on ferrite substrate in TM_{mn} mode are calculated by modifying the relations proposed by Lee *et al* [12]. The modified expressions are :

$$f_r = \frac{2c\sqrt{\mu_0}}{\cdot}\sqrt{m^2+mn+n^2} \tag{7}$$

$$Z_{in} = -i\omega\mu_0\sum_{n=1}^{1}\sum_{m=n}^{1} 4\sqrt{3}hA'_{mn}\cos\left(\frac{2\pi nd}{\sqrt{3}a}\right)\frac{\sin\left(\frac{2\pi mw}{\sqrt{3}a}\right)}{\left(\frac{2\pi mw}{\sqrt{3}a}\right)}$$

$$+\cos\left(\frac{2\pi nd}{\sqrt{3}a}\right)\left(\frac{\sin\left(\frac{2\pi mw}{\sqrt{3}a}\right)}{\left(\frac{2\pi mw}{\sqrt{3}a}\right)}\right)$$

$$+\cos\left(\frac{2\pi nd}{\sqrt{3}a}\right)\left(\frac{\sin\left(\frac{2\pi mw}{\sqrt{3}a}\right)}{\left(\frac{2\pi mw}{\sqrt{3}a}\right)}\right)^2$$

$$\times\left[\frac{(\omega^2-\varpi_r^2)\mu_0\varepsilon_0\varepsilon_r+i\delta_{eff}k^2}{\left[(\omega^2-\varpi_r^2)\mu_0\varepsilon_0\varepsilon_r\right]^2+\left[\delta_{eff}k^2\right]^2}\right] \tag{8}$$

Here, A'_{mn} is equal to 6 when $m = n \neq 0$ and 'd' is feed point location on the patch. δ_{eff} is the effective loss tangent. The coaxial feed can be modeled by considering a current ribbon of effective width '$2w$' along the z-axis [10]. The value of 'w' should be so chosen that best fitting with experimental results might be obtained. Usually this effective width is several times larger than the physical diameter of the inner conductor of coaxial feed; still the input impedance is not a sensitive function of '$2w$'. The value of '$2w$' used for present computation is 0.006 meter.

The change in effective permeability (μ_{eff}) of substrate material with applied bias magnetic field (H_0) also changes the resonance frequency (f_r) of antenna, which in turn affects its input impedance. The variation of computed real input impedance of ETMA structure with frequency is shown in Figure 3. In the absence of bias magnetic field ($H_0 = 0$), the resonance frequency of structure in TM_{11} mode is 1.237 GHz. In the presence of applied bias magnetic field,

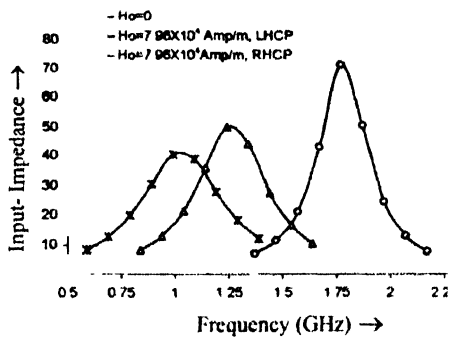

Figure 3. Variation of real input impedance with frequency for biased and unbiased conditions

resonance curve shifts in opposite directions for RHCP and LHCP modes. This variation is shown in Figure 3 for $H_0 = 7.96 \times 10^4$ amp/m. The resonance frequency for RHCP mode approaches to 0.992 GHz, which indicates that overall size of the patch will reduce for operation of antenna at the same frequency. In contrary, resonance frequency for LHCP mode approaches to 1.766 GHz, which suggest a reverse

result with regards to overall patch size for LHCP mode. On further increasing the DC bias field (as shown in Figure 4 for $H_0 = 2.39 \times 10^5$ Amp/m), resonance curves for RHCP and LHCP modes come closer. This result is again shown in Figure 5 where the variation of resonance

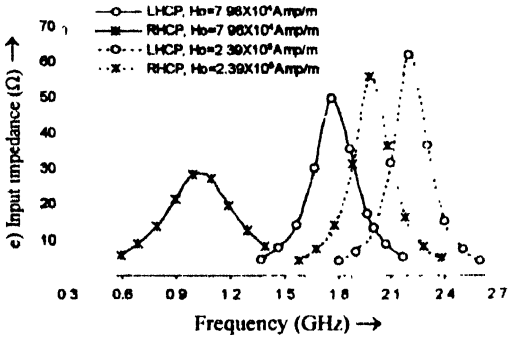

Figure 4. Variation of real input impedance with frequency under biased condition.

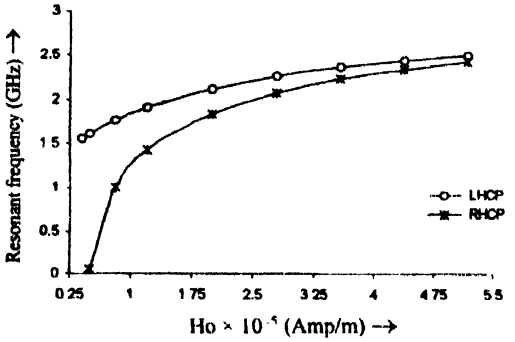

Figure 5. Variation of resonance frequency with applied bias field in TM_{11} mode of excitation.

frequency with applied DC bias field is shown. From Figure 5, it is also observed that with RHCP waves, resonance frequency of antenna decreases sharply near 'off switch' condition *i.e.* when applied bias field approaches close to 4.98×10^4 Amp/meter. The effect of magnetic bias field on resonance frequency for LHCP mode is quite weak however frequency tunability of RHCP mode is significantly large as compared to LHCP mode.

The variation of computed real input impedance of antenna as a function of applied bias field is shown in Figure 6. The effect of applied bias field on input impedance

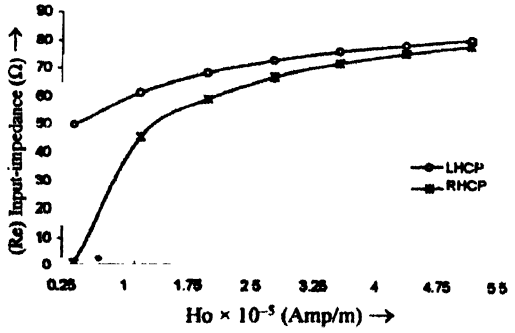

Figure 6. Variation of input impedance of antenna with applied bias field in TM_{11} mode of excitation.

of antenna in LHCP mode is significantly weaker than that in RHCP mode. Input impedance of antenna in the case of LHCP mode with feed location (0.00672 m, 0), varies from 50.07 to 80.4 Ω. This indicates that antenna can operate in entire range of magnetic field without many reflections. However in the case of RHCP mode with same feed location, a large variation in input impedance is obtained which indicates that antenna can now operate in a limited range of magnetic field *i.e.* from $H_0 = 2.00 \times 10^5$ Amp/m to 5.71×10^5 Amp/m.

By applying the concept of equivalent sources and image theory, the surface magnetic current density (M) is evaluated which in tern is used to find vector electric potential (F) given by :

$$F = \frac{\varepsilon_0}{4\pi} \int M \frac{e^{-jkR}}{R} ds \tag{9}$$

$$\text{with } M = 2(E \times \hat{n}). \tag{10}$$

Expressions for far zone field components (E_θ and E_ϕ) are derived by computing components of surface current density (M) at different edges of the patch and vector electric potential (F) *i.e.*

$$E_\theta = -j\omega\eta\left[F_x \cos\theta\cos\phi + F_y \cos\theta\sin\phi\right], \tag{11}$$

$$E_\phi = +j\omega\eta\left[F_x \sin\phi - F_y \cos\phi\right]. \tag{12}$$

Using equations (11) and (12) and a mathematical software Math CAD Plus 6.0, the far zone field pattern factors $R_{th} = \eta^2\omega^2(|E_\theta|^2 + |E_\phi|^2)$ are computed in $E(\phi = 0)$ and $H(\phi = \pi/2)$ planes for TM_{11} mode of excitation. In Figure 7, E and H plane radiation pattern factors of ETMA

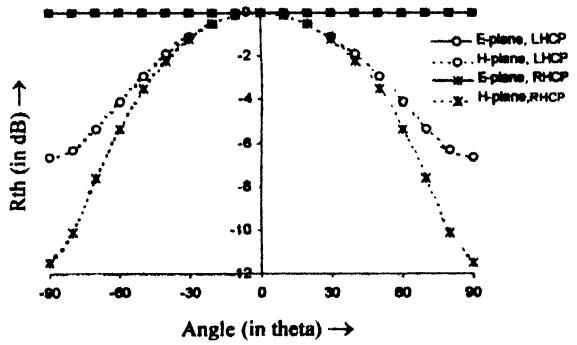

Figure 7. Radiation pattern of ETMA structure in E and H planes under biased condition.

structure on ferrite substrate are shown for both LHCP and RHCP waves. As shown in figure, E plane patterns for both LHCP and RHCP waves are nearly ominidirectional. However, H plane pattern indicates that 3 dB beam width with LHCP waves is little larger than that with RHCP waves. This behavior is again shown in Figure 8 where directivity of ETMA structure is plotted as a function of applied magnetic field. For all values of applied bias field, directivity

of antenna with RHCP waves is little higher than that with LHCP waves. However in both the cases, directivity of antenna decreases with increase in applied bias field.

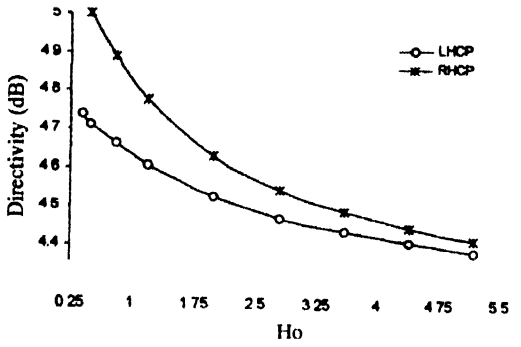

Figure 8. Variation of directivity of antenna with applied bias field in TM_{11} mode of excitation.

The effect of applied magnetic field on bandwidth (BW) and quality factor (Q_T) of ETMA structure are shown in Figures 9 and 10 respectively. The bandwidth of antenna increases marginally on increasing applied bias field. For all the values of applied bias, the bandwidth of antenna with LHCP waves is little larger than that with RHCP waves. When applied bias field approaches closer to 4.98×10^4 Amp/meter (just above 'off switch' condition), a sharp decrease in bandwidth of antenna with RHCP waves is found.

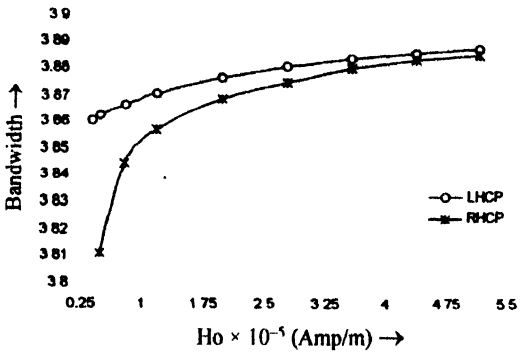

Figure 9. Variation of bandwidth of antenna with applied bias field in TM_{11} mode of excitation.

The computed bandwidth of ETMA structure built on ferrite substrate is significantly larger than that built on pure dielectric substrate (Table 2). The total quality factor of antenna (Q_l), which includes dielectric, magnetic, conductor and radiation losses, is computed as a function of applied bias field and is shown in Figure 10. It is evident from this

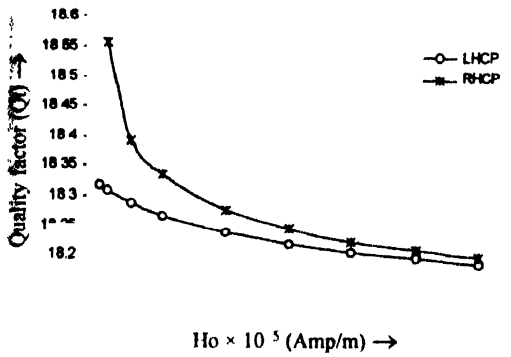

Figure 10. Variation of total quality factor of antenna with applied bias field in TM_{11} mode of excitation.

figure that total quality factor of antenna decreases significantly with increase in applied bias field. Since angular frequency (ω), radiated power by antenna (P_r), relative permeability μ_{eff} of substrate and total stored energy in the cavity (W_T) are involved in the expression of total quality factor and each of them is a sensitive function of applied bias field, perhaps their combined effect is responsible for minor decrease in Q_l with applied bias field.

The radiation characteristics of ETMA structure printed on ferrite substrate as well as on pure dielectric substrate ($\varepsilon_r = 2.32$, $\tan\delta = 0.001$) are compared in Table 2. Keeping patch size equal in both the cases, resonance frequency of antenna on pure dielectric substrate is found much larger than that on ferrite substrate. The directivity of antenna printed on ferrite substrate is little larger than that of antenna printed on pure dielectric substrate. However, a large difference in bandwidth and total quality factor of antenna is recorded. The bandwidth of antenna on ferrite substrate

Table 2. Comparison between radiation properties of ETMA structure printed on pure dielectric substrate and ferrite substrate in TM_{11} mode.

		Patch-edge dimension (a) (meters)	Resonant frequency (GHz)	Quality factor (Q_l)	Band-width (%)	Directive Gain (in dB)
Ferrite substrate						
$\varepsilon_r = 15$	LHCP	0.030	1.766	18.289	3.866	4.661
$h = 0.002$ meter						
$\mu_0 M_s = 0.3$ Tesla						
$H_0 = 7.96 \times 10^4$ Amp/m	RHCP	0.030	0.993	18.393	3.845	4.888
$\tan\delta = 0.0476$						
Pure dielectric substrate						
$\varepsilon_r = 2.32$, $h = 0.0016$ meter		0.030	7.319	82.933	0.853	4.354
$\tan\delta = 0.001$						

is significantly larger than that on pure dielectric substrate. In contrary, the total quality factor of antenna printed on pure dielectric substrate is much larger than that on ferrite substrate.

3. Conclusions

The radiation properties of an ETMA structure printed on a ferrite substrate are studied theoretically in this paper by considering presence of bias magnetic field in the direction of propagation of *e.m.* waves. The bandwidth of antenna under the present condition is found sufficiently larger than that of a similar antenna built on pure dielectric substrate having no magnetic properties. A better tunability can be obtained by printing an ETMA structure on ferrite substrate. Since a triangular geometry has physically smaller area than that of a rectangular geometry and radiation properties of these two structures are comparable, ETMA structures may be proved a better choice than a rectangular microstrip antenna for application in phased array design particularly in switchable array design. The work reported in this paper is of theoretical nature and requires experimental verification. However, these results could not be verified at our center due to limitations in experimental facilities and non-availability of ferrite substrate.

References

[1] R E Collin in *Foundations for Microwave Engineering* (New York : McGraw Hill) 450 (1992)

[2] K K Tsang and R J Langley *IEE Proc. Microwave Antennas Propag.* **145** 49 (1998)

[3] R E Post and D T Stephenson *IEEE Trans.* **AP-29** 129 (1981)

[4] N Das and S K Chowdhary *Electron Lett.* **16** 817 (1980)

[5] R E Collin in *Field Theory of Guided Waves* (New York : McGraw Hill) (1960)

[6] J V Bladel *IRE Trans.* **AP-9** 563 (1961)

[7] J G Fikioris *J. Math. Phys.* **6** 1617 (1965)

[8] S W Lee, J Boersma, C L Law and G A Deschamps *IEEE Trans.* **AP-28** 331 (1980)

[9] D S Jones in *Methods in Electromagnetic Wave Propagation* (Oxford : Clarendon) (1979)

[10] J R James and P S Hall in *Hand Book of Microstrip Antennas* (London : Peter Peregrinus Ltd.) **Ch 3** (1989)

[11] N E Buris, T B Funk and R S Solverstein *IEEE Trans.* **AP-41** 165 (1993)

[12] K F Lee, K M Luk and J S Dahele *IEEE Trans.* **AP-36** 1510 (1988)